Iraqi Journal of Physics, 2019 *Vol.17, No.40, PP. 21-32*
DOI: 10.20723/ijp.17.40.21-32

Enhancement of NO_2 gas sensing behavior for ZnS/PPy nanostructure by loading graphene

Sabreen A. Khalaf and Iftikhar M. Ali

Department of Physics, College of Science, University of Baghdad

E-mail: iftikhariq@gmail.com

Abstract

The pure ZnS and ZnS-Gr nanocomposite have been prepared successfully by a novel method using chemical co-precipitation. Also conductive polymer PPy nanotubes and ZnS-PPy nanocomposite have been synthesized successfully by chemical route. The effect of graphene on the characterization of ZnS has been investigated. X-ray diffraction (XRD) study confirmed the formation of cubic and hexagonal structure of ZnS-Gr. Dc-conductivity proves that ZnS and ZnS-Gr have semiconductor behavior. The SEM proved that formation of PPy nanotubes and the Gr nanosheet. The sensing properties of ZnS-PPy/ZnS-Gr for NO_2 gas was investigated as a function of operating temperature and time under optimal condition. The sensitivity, response time and recovery time were calculated with different operating temperatures.

Key words
ZnS, graphene, PPy, nanocrystals, structural and electrical properties, gas sensor.

Article info.
Received: Sep. 2018
Accepted: Oct. 2018
Published: Mar. 2019

تحسين السلوك التحسسي لغاز NO_2 للتركيب النانوي ZnS/PPy بإضافة الكرافين

صابرين علي خلف و افتخار محمود علي

قسم الفيزياء، كلية العلوم، جامعة بغداد

الخلاصة

تم تحضير كبريتيد الزنك النقي وكبريتيد الزنك مع الكرافين بواسطة الترسيب الكيميائي، كذلك تم تحضير بولي بايرول النقي وبولي بايرول مع كبريتيد الزنك بواسطة الترسيب الكيميائي. اكدت دراسة حيود الأشعة السينية تكوين كبريتيد الزنك بطوره المكعب وبعد اضافه الكرافين تم تكوين الطور السداسي بالاضافه الى المكعب. اكدت نتائج توصيلية التيار المستمر سلوك شبه موصل لكل من الكرافين و كبريتيد الزنك. أثبتت دراسة المجهر الالكتروني الماسح تكوين الأنابيب النانوية لبولي بايرول و الالواح النانوية للكرافين. تم دراسة خصائص الاستشعار لكبريتيد الزنك-بولي بايرول-الكرافين تجاه غاز NO_2 كدالة لدرجة حرارة التشغيل والوقت. تم حساب التحسسية وزمن الصعود والنزول مع درجات حرارة مختلفة.

Introduction

Recent studies have converge on sensing gases such as CO, CO_2, SO_2, O_3, H_2 and NH_3 in the atmosphere. A sensor is a device that can measure a physical parameter and transform it to an electrical signal. Physical parameters include temperature, light, velocity, as well as biological and chemical concentrations. Sensors that are designed to detect harmful or toxic gases need to be designed such that they are accurate, sensitive and rapid. Gas sensors are important for detecting and/or monitoring hazardous gases that exist in small concentrations [1].

Zinc sulfide (ZnS) is a II-VI semiconductor. This material happen naturally in the two various crystal structures Zincblende and wurtzite, which are cubic and hexagonal structures, respectively [2]. The Zincblende structure is the most steady structure at room temperature, and it

convert into wurtzite at 1020 ^{o}C [3]. In both structures each Zn atom is connected to four S atoms in a tetrahedral arrangement, with a mixed bonding of covalent and ionic binding forces between the atoms [4]. The rising amount of ionic bonds in the semiconductor would lead to an increase of the inter elemental forces, which in turn could command to shorter distances between the atoms. As a result, the crystal structure would alteration from Zincblende to wurtzite. Since the energy gap increases with the amount of ionic bonds in a semiconductor, this could clear why the band gap is crystal structure dependent [5]. Graphene nano sheet (GNS) is one layer of graphite. graphene possesses singular physical properties, its two dimensional planar structure, half metallicity, and high electron mobility. All these electronic and structural properties of the GNS make it a promising route to use it in several applications, such as nano-electronics, solid state sensors, and spintronic [6-8]. More recently, graphene, has been known to be a promising sensing material as a result of its distinctive and wonderful electrical and mechanical properties [9]. Hyeun Joong Yoon et al., G. Ko et al., studied the graphene sensing against CO_2 and NO_2 gases [9, 10]. Polypyrrole (PPy), one of the most extensively investigated conducting polymers, has attracted a great deal of interest because of its good electrical conductivity, environmental stability and easy synthesis. PPy has been performed in a number of implementation, such as batteries, supercapacitors, sensors, microwave shielding and corrosion protection [11]. Nowadays there is a great interest in making conducting polymer sensors. polypyrrole has been widely used as an effective material for the detection of toxic, hazardous and flammable gases. Dunst et al. [12] studied PPy against toxic gas NH_3.

In this work, the sensing properties for ZnS/PPy will be improved by loading Graphene to detect NO_2 toxic gas.

Experimental details

Synthesis of ZnS and ZnS-Gr nanocomposite

ZnS nanoparticles were synthesized by co-precipitation chemical method**.** A stock solution of Zn^{2+} was prepared by adding 0.1 M of $Zn(NO_3)_2.6H_2O$ into 50mL of distilled water. A stock solution of S^{2-} was prepared by adding 0.2 M of Na_2S into 50mL of distilled water. Then put the first solution on magnetic stirrer at temperature of 80^{o}C for 1 hr, then the second solution is added drop wise and the whole solution is stirred for 30 min. Milky precipitation will be observed that indicates ZnS formation, then filtered and washed several times using distilled water, ethanol and finally by acetone then dried using oven at 100 ^{o}C for 5 hr. For preparing Zinc sulfide with Graphene (ZnS-Gr), the different volume ratios (5, 10, 20)% of Graphene (Gr) was added to stock solution of Zn^{2+} and stirred together at 80^{o}C for 1 hr, then solution of S^{2-} is added drop wise and the whole solution is stirred for 30 min. Grey color precipitation will be observed that indicates ZnS-Gr formation, then filtered and washed several times using distilled water, ethanol and finally by acetone then dried using oven at 100 ^{o}C for 5 hr.

Synthesis of polypyrrole (PPy) and ZnS-PPy nanocomposite

Polypyrrole (PPy) nanotubes were prepared by the following method reported by An et al. [13]. 2 mM of methyl orange and 20 mM of $FeCl_3$ were dissolved in 500 ml of distilled water, followed by the addition of 0.84

ml pyrrole monomer with stirring for 24 h. The as-prepared sample was filtered and washed with distilled water several times and then dried at 100 °C for 6 h.

ZnS-PPy composite was synthesized by chemical method. A stock solution of Zn^{2+} was prepared by adding 0.5 mM of $Zn(NO_3)_2$.6H2O into 50 mL of distilled water. A stock solution of S^{2-} was prepared by adding 10 mM of Na_2S into 50mL of distilled water. Then adding 5mL of ppy to first solution and put them on magnetic stirrer at temperature of 80 °C for 1 hr, then the second solution is added drop wise and the whole solution is stirred for 30 min. Then filtered and washed several times using distilled water, ethanol and finally by acetone then dried using oven at 100 °C for 5 hr.

Preparation of ZnS-Gr-PPy

The preparation of ZnS-PPy/ZnS-Gr by using Chemical spray pyrolysis Method (c.s.p). Here are the basic steps to the process of the preparation of films:

The solutions put on the magnetic stirrer for about 15 minutes to ensure that the mixture solutions are mixed properly. Then the solution must be put in sprayer container. The glass substrate was heated and left until they reach the desired temperature. The solution (ZnS-PPy) sprays on glass substrate, then the second solution (ZnS-Gr) spray above the first solution. After that the films Zns-PPy/ZnS-Gr were gotten. During the operation of spraying, the glass substrate must be moved regularly and the amount of spray should be controlled to get the best homogeneity of the films. After the spray process completed, then the hot plate will be shut down and the samples are left on the surface of the heater to reach the room temperatures, then the substrates can be raised.

Results and discussion

1- Structural properties

1-1 X-Ray diffraction analysis results

Fig.1 shows the x-ray diffraction of ZnS/Gr at different volume ratios of Gr which are (5, 10, 20) %. From figure (1a) it has been observed that pure ZnS has cubic zinc blende structure with comparison to the standard card ICDPDS (96-110-1051). The three main peaks are observed in the diffractrogram at 2Θ equal 28.3549, 47.5354, 56.195 corresponds to (111), (220) and (311) planes respectively. For the ZnS/Gr system with different volume addition ratios (5, 10, 20) % of Gr, ZnS is still with cubic structure at 5% Gr volume ratio as shown in figure (1b). More addition of graphene which are (10, 20) % as shown in Figure (1c,d,), new phase for ZnS appeared that is hexagonal structure with comparison to the standard card ASTM (I2-688) because Gr sheet has Hexagon structure (honeycomb lattice), so the graphene sheet becomes as a template to ZnS growth on this sheet. In the same time, graphene peaks will appear at ZnS/10% Gr but very slight as in figure (1c) and more Gr addition, Gr peaks will be distinguished as shown in figure (1d), so high Gr addition activate the presence of ZnS hexagonal phase beside ZnS cubic phase.

The data of peaks positions and miller indices for the diffracted planes, FWHM and crystallite size are shown in Table 1. The interplaner spacing d is calculated using the relation

$$d_{hkl} = n\lambda / 2\sin\Theta$$

where λ is the X-ray wavelength (here λ = 1.54184 Å) and θ is the Bragg angle. The average crystallite size is calculated from Scherer formula

$$D=0.9\lambda/(\beta \cos\theta)$$

where β is the full-width at half-maximum (FWHM) measured in radian.

1-2 SEM analysis results

Scanning electron microscopy (SEM) is a versatile technique for studying morphology of materials. The images of pure ZnS, as shown in Fig.2(a) prepared by co-precipitation route without adding the Graphene (Gr) which has nano size with nanoparticle structure where ZnS nanoparticles tend to aggregate without the dispersion of Graphene. Fig.2 (b) illustrates the images of Gr which have nanosheet shape. For the polymer polypyrrole (PPy), SEM images prove the formation of nanotubes structure as shown in Fig.2 (c) with diameter less than 100 nm. ZnS with Gr nano powder are shown in Fig.2 (d) and it is clear that ZnS nanoparticles are loaded on Graphene nanosheet.

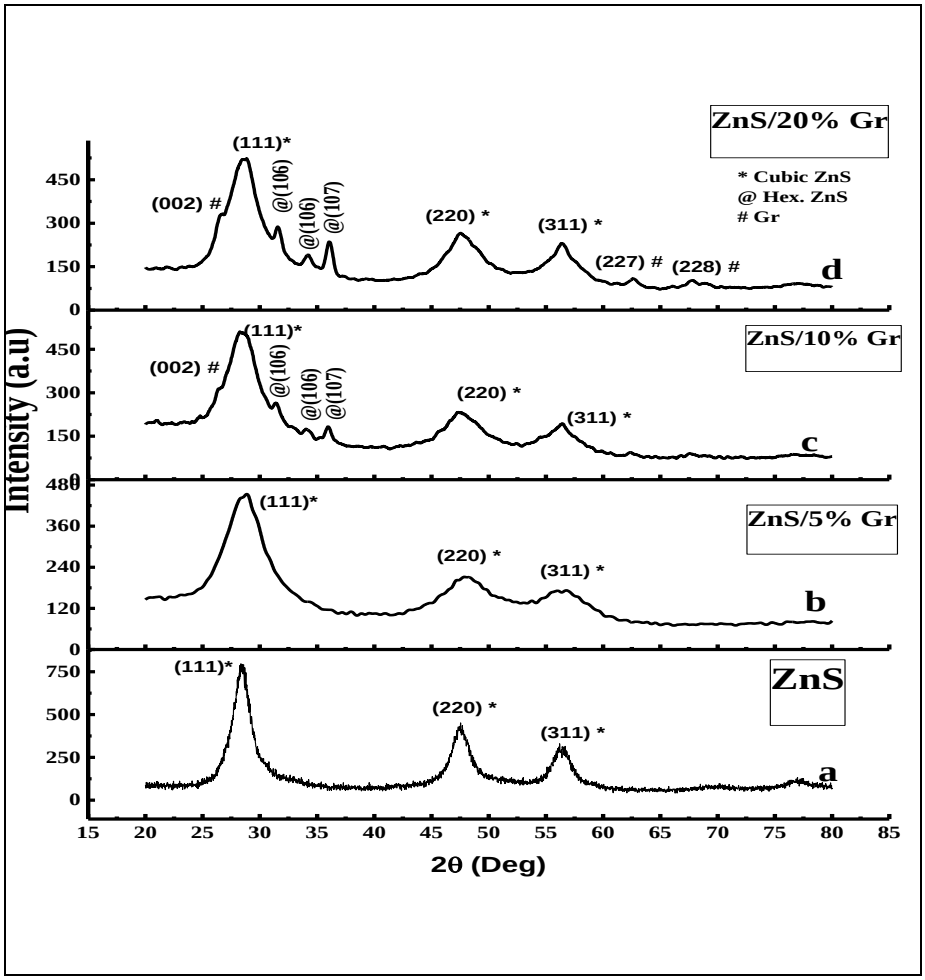

Fig.1: XRD patterns for ZnS-Gr at different volume ratios of Gr.

Table 1: Structural parameters of ZnS-Gr nanocomposite which are diffraction angle (2θ), (hkl), d-spacing, and FWHM

% Gr	2Θ (deg)	Interplant spacing d (Å)	FWHM (Rad)	Plane (hkl)	D Crystalline size (nm)	Average size (nm)	element	Phase	Card no.
0	28.3549 47.5354 56.195	3.147897 1.912953 1.63712	0.043611 0.034889 0.027911	111 220 311	3.281995 4.34635 5.636229	4.4213	ZnS	Cubic Cubic Cubic	96-110-1051 5-0566 96-110-1051
5	28.7191 47.8389 56.4985	3.108548 1.901628 1.628819	0.087222 0.104667 0.087222	111 220 311	1.642349 1.450357 1.806248	1.632	ZnS	Cubic Cubic Cubic	96-110-1051 5-0566 96-110-1051
10	28.4358 31.4505 34.0808 35.9826 47.4343 56.3973	3.138925 2.844723 2.631126 2.496503 1.916758 1.631577	0.066289 0.027911 0.020933 0.013956 0.087222 0.095944	111 106 106 107 220 311	2.413724 5.1654 6.962405 10.45435 1.737786 2.26613	4.832	ZnS	Cubic Hex Hex Hex Cubic Cubic	96-110-1051 I2-688 I2-688 I2-688 5-0566 96-110-1051
20	26.6351 28.6179 31.5314 34.1819 36.0635 47.5354 56.3367 62.6492 67.7479	3.34746 3.11987 2.837394 2.623962 2.490856 1.912953 1.633305 1.482595 1.383312	0.024422 0.052333 0.020933 0.024422 0.017444 0.069778 0.055822 0.022678 0.017444	002 111 106 106 107 220 311 227 228	5.839009 2.736683 6.916823 5.944541 8.36634 2.173182 2.820021 7.163442 7.973054	5.547	Gr ZnS Gr Gr	Hex cubic Hex Hex Hex Cubic Cubic Hex Hex	23-64 96-110-1051 I2-688 I2-688 I2-688 5-0566 96-110-1051 22-1069 22-1069

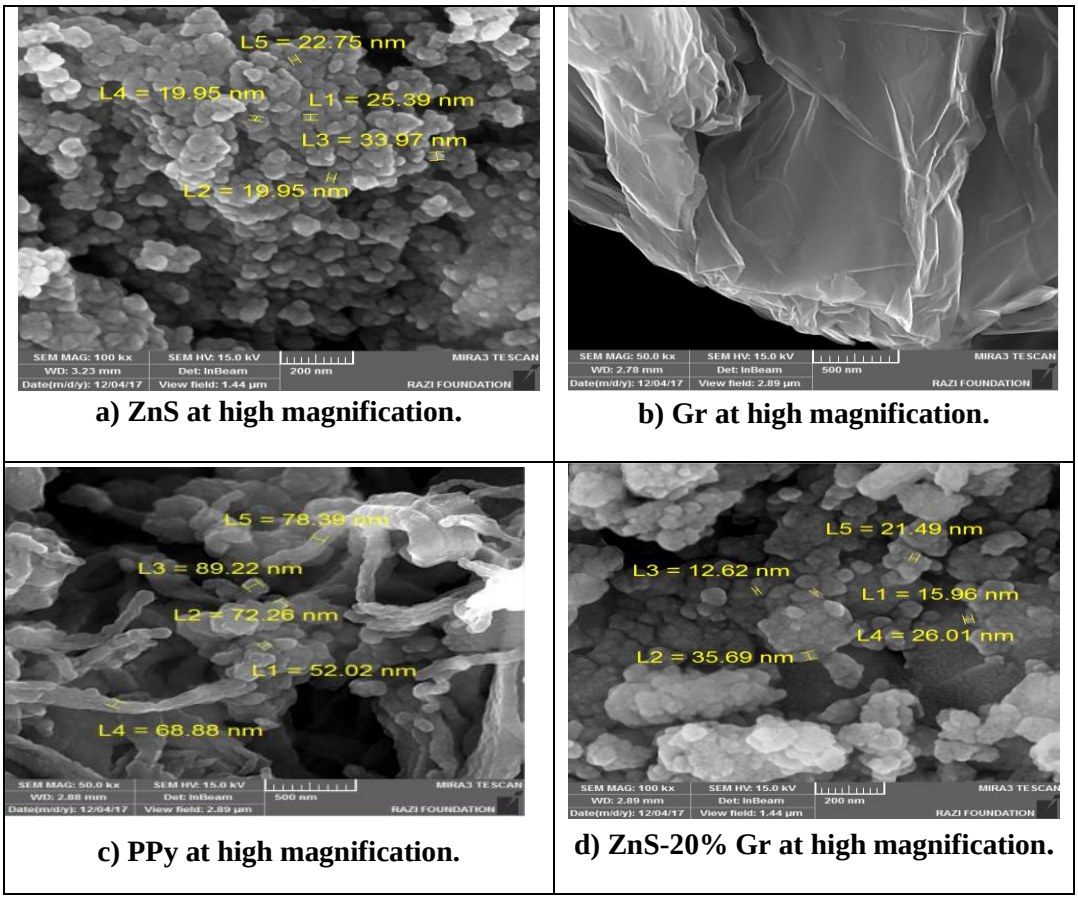

a) ZnS at high magnification.

b) Gr at high magnification.

c) PPy at high magnification.

d) ZnS-20% Gr at high magnification.

Fig.2: SEM images of pure a) ZnS, b) Gr , c) PPy and d) ZnS-Gr.

2 Electrical properties

2.1 DC-measurement of ZnS/Gr

The dc-conductivity ($\sigma_{d.c}$) for pure ZnS and ZnS/Gr at different volume ratios of Gr is studied as a function of temperature with the range of (303-473) K as shown in Fig.3(a). Dc-conductivity proves that ZnS and ZnS-Gr have semiconductor behavior because these samples have negative temperature coefficient. One can see that after PPy addition, activation energy decreases, this may be because PPy conductive polymer creates localized states inside band gap for the composites which is ZnS-Gr as seen in Fig.3(b).

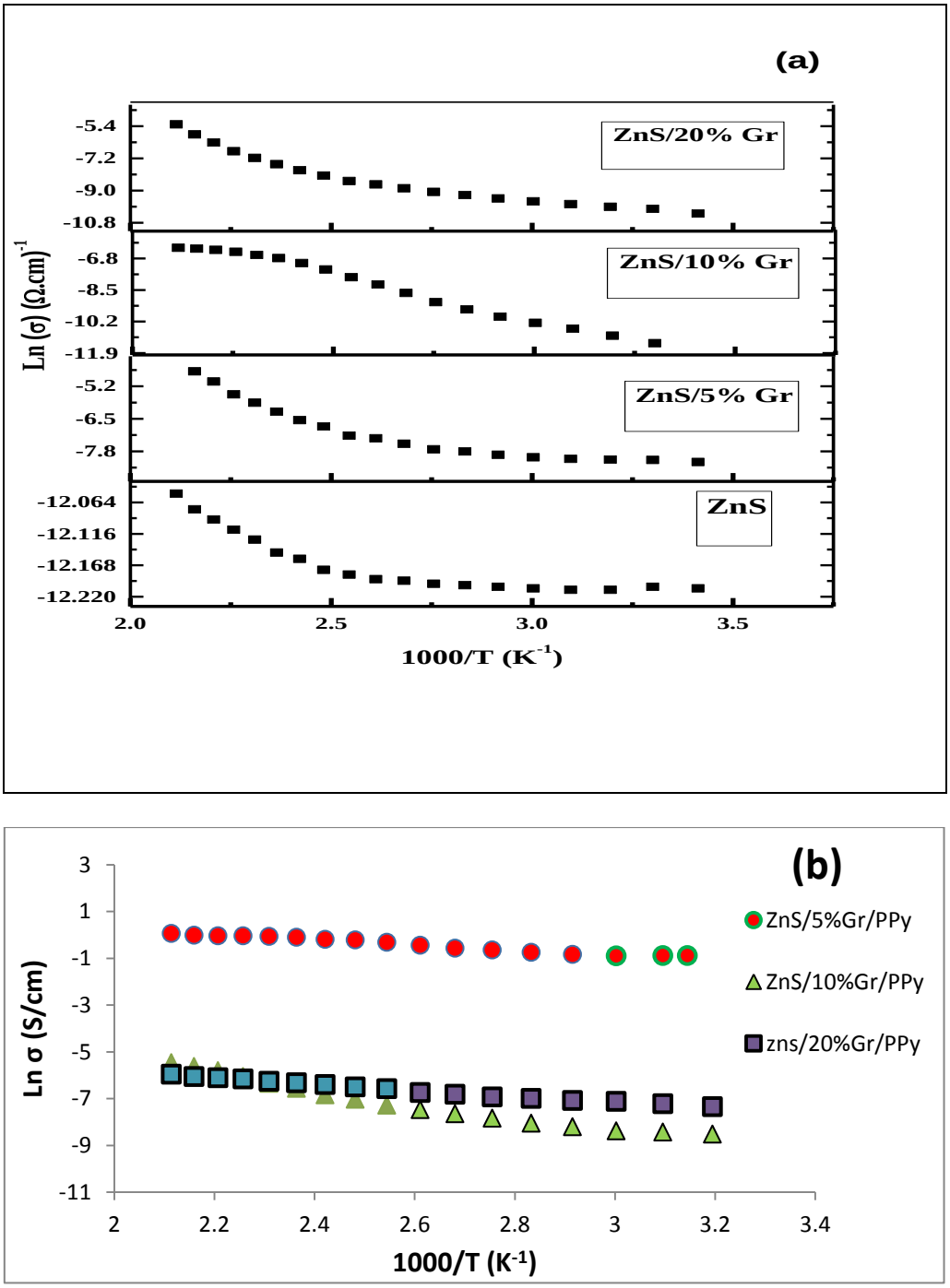

Fig.3: Temperature dependence of dc-conductivity of the deposited (a)ZnS-Gr and (b) ZnS-Gr-PPy thin films.

Table 2: D.C. Conductivity Parameters for pure ZnS and ZnS with different volume ratio (5, 10, 20)% of Gr.

% Gr	ZnS-Gr		ZnS-Gr-PPy	
	$E_{a\,1}$ (eV)	$E_{a\,2}$ (eV)	$E_{a\,1}$ (eV)	$E_{a\,2}$ (eV)
0	0.001	0.026	0.001	0.026
5	0.063	0.518	0.0049	0.1188
10	0.088	0.553	0.158	0.375
20	0.167	0.623	0.085	0.122

3- Gas sensing measurement against NO_2 toxic gas

Thin films specimens are examined for gas sensing using NO_2 toxic gas at different operation temperatures. The sensitivity factor (S%) for n-type material and oxidizing gas is calculated by equation [14]

$$S=|(R_g-R_a) / R_g |*100\%$$

where S is the sensitivity, R_a and R_g are the electrical resistance of the film in the air and electrical resistance of the film in the presence of gas, respectively.

Figs. 4-9 include the sensitivity of ZnS, Gr and ZnS-PPy/ZnS-Gr against NO_2 gas. Loading conductive polymer PPy to ZnS and to ZnS-Gr system that also make thin films being sensitive for input gas because ZnS nanoparticles which acts as catalyst will spread along the polypyrrole nanotubes also the surface area of PPy nanotube makes good area to adsorb input gas so sensitivity has been improved. Also conductive polymer such as PPy nanotubes represent bath to carriers to follow and reach electrodes and record electric current and the values of sensitivity and response and recovery times are shown in Table 3 and 4.

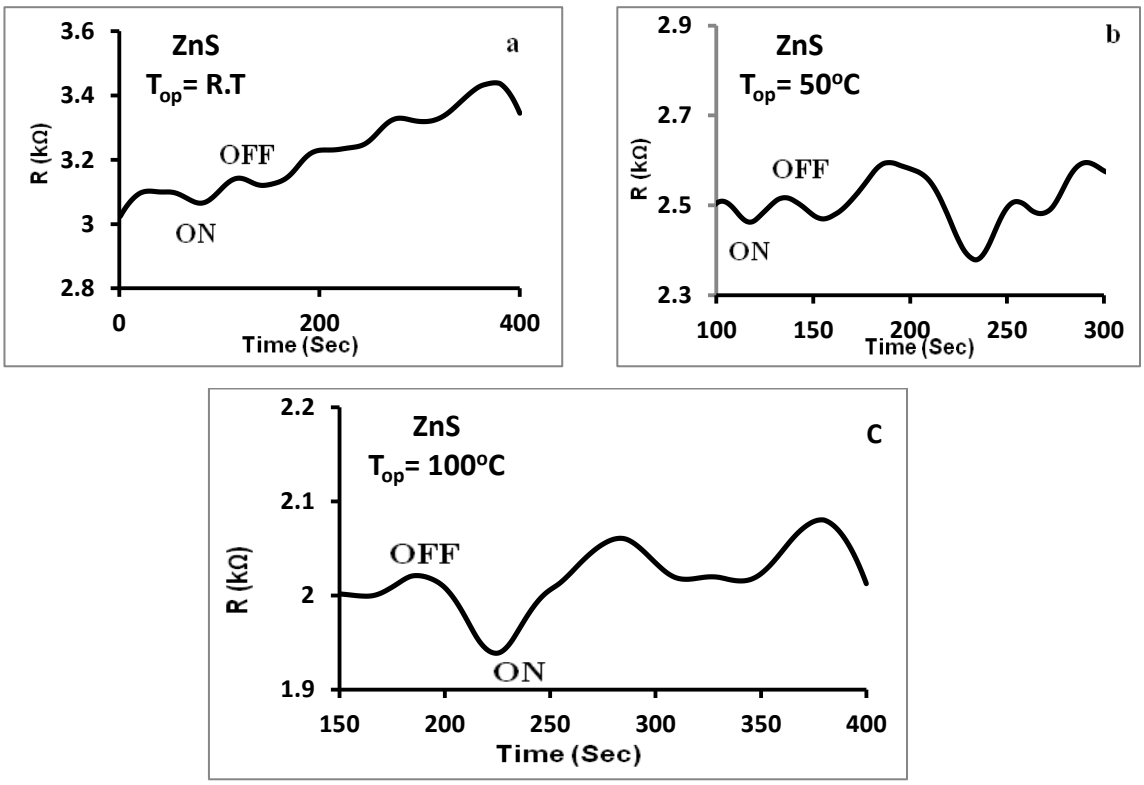

Fig.4: The variation of resistance with time for pure ZnS against NO_2 gas at operating temperatures: a) R.T; b) 50 °C and c) 100 °C.

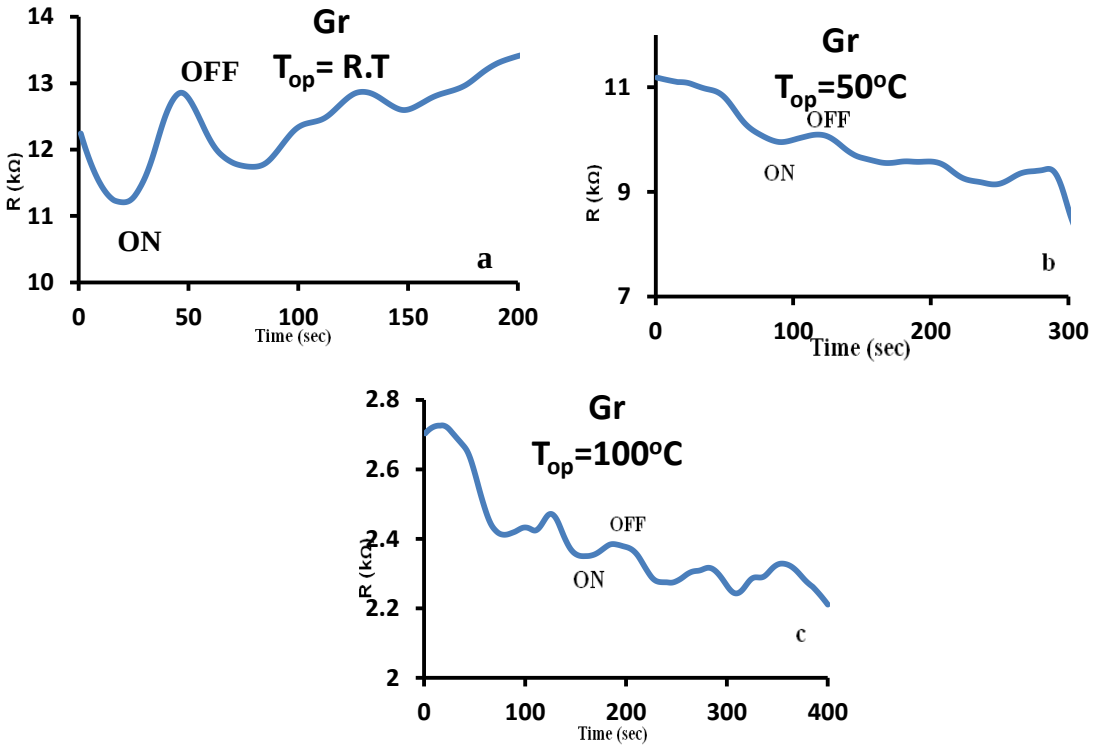

Fig.5: The variation of resistance with time for Gr at different operating temperatures against NO_2 gas.

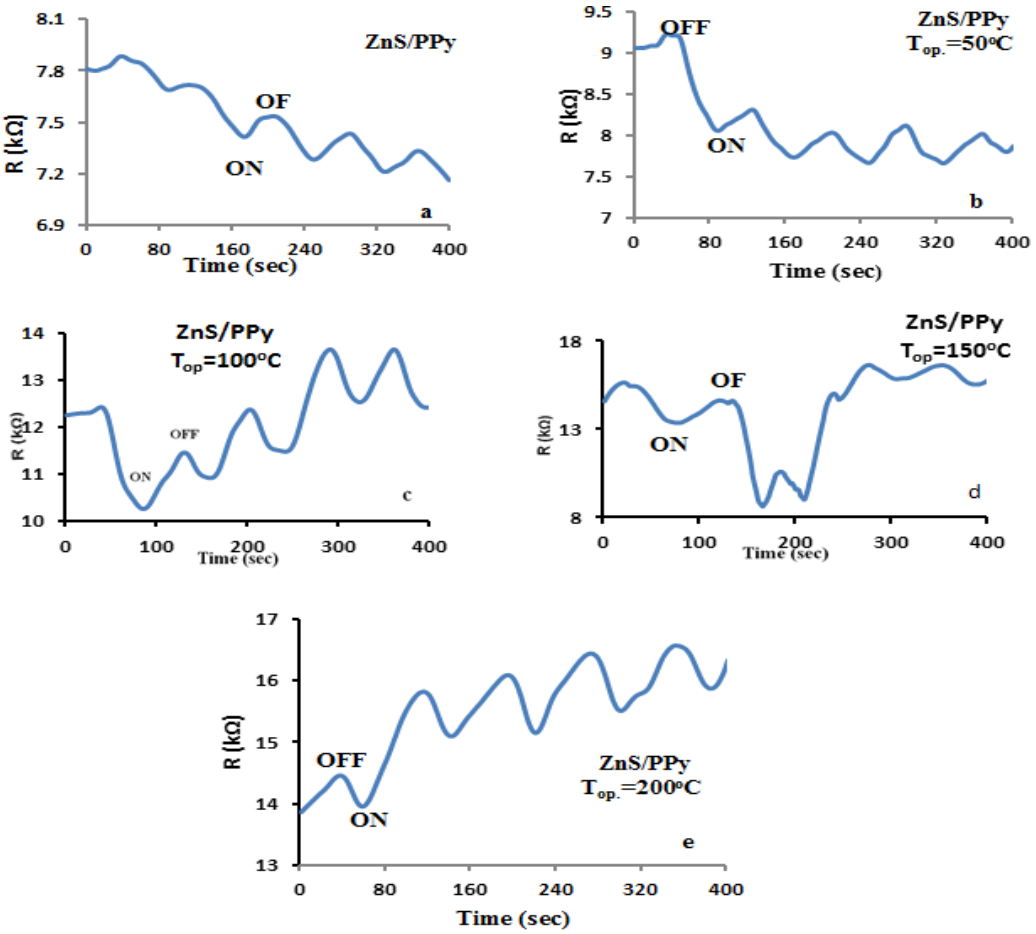

Fig.6: The variation of resistance with time for ZnS-PPy at different operating temperatures against NO_2 gas.

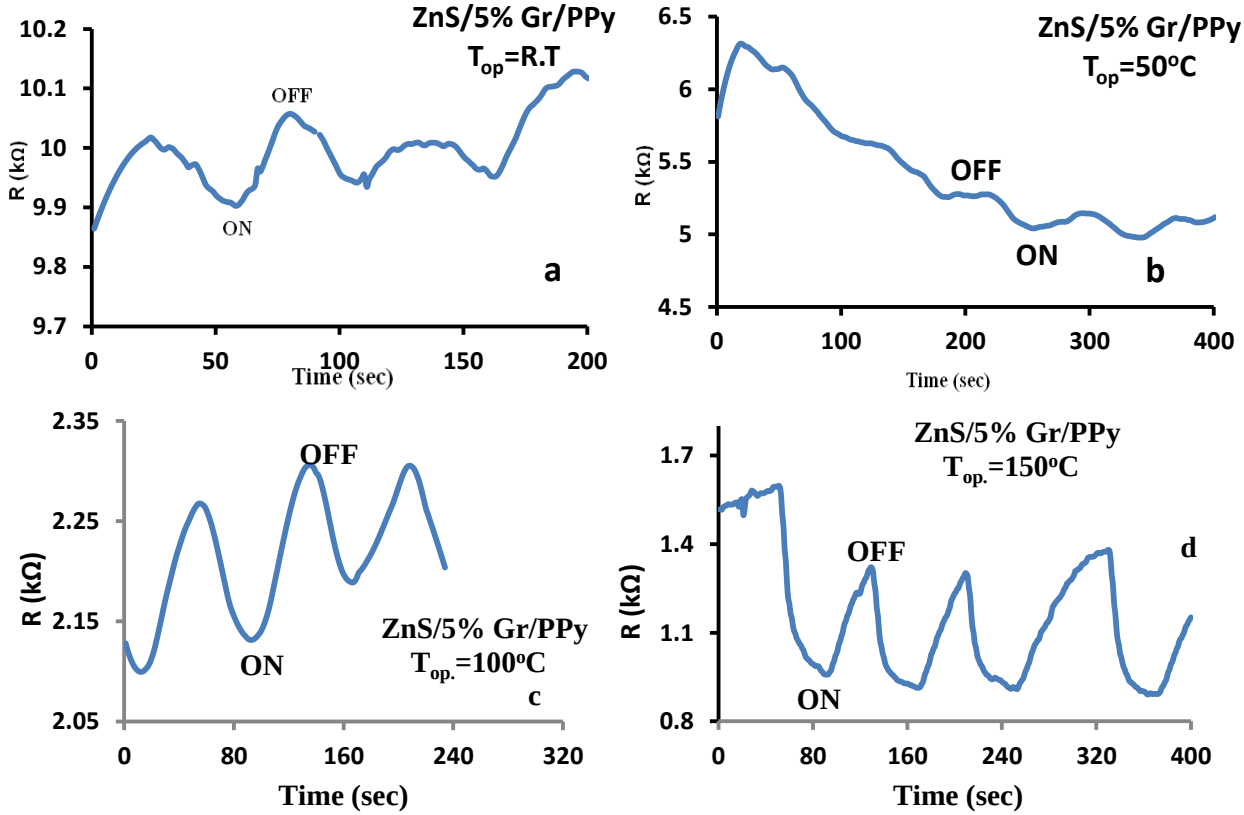

Fig.7: The variation of resistance with time for ZnS/5% Gr/PPy at different operating temperatures against NO_2 gas.

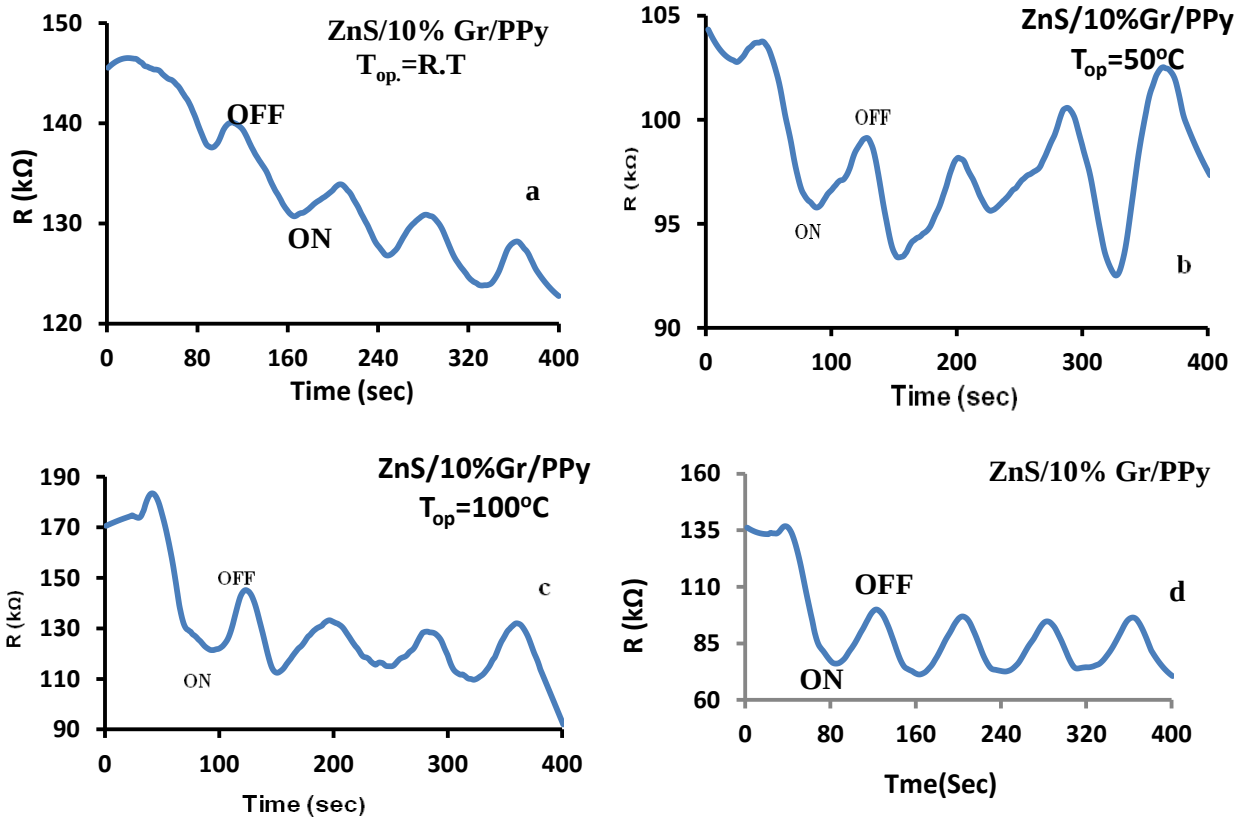

Fig.8: The variation of resistance with time for ZnS/10% Gr/PPy at different operating temperatures against NO_2 gas.

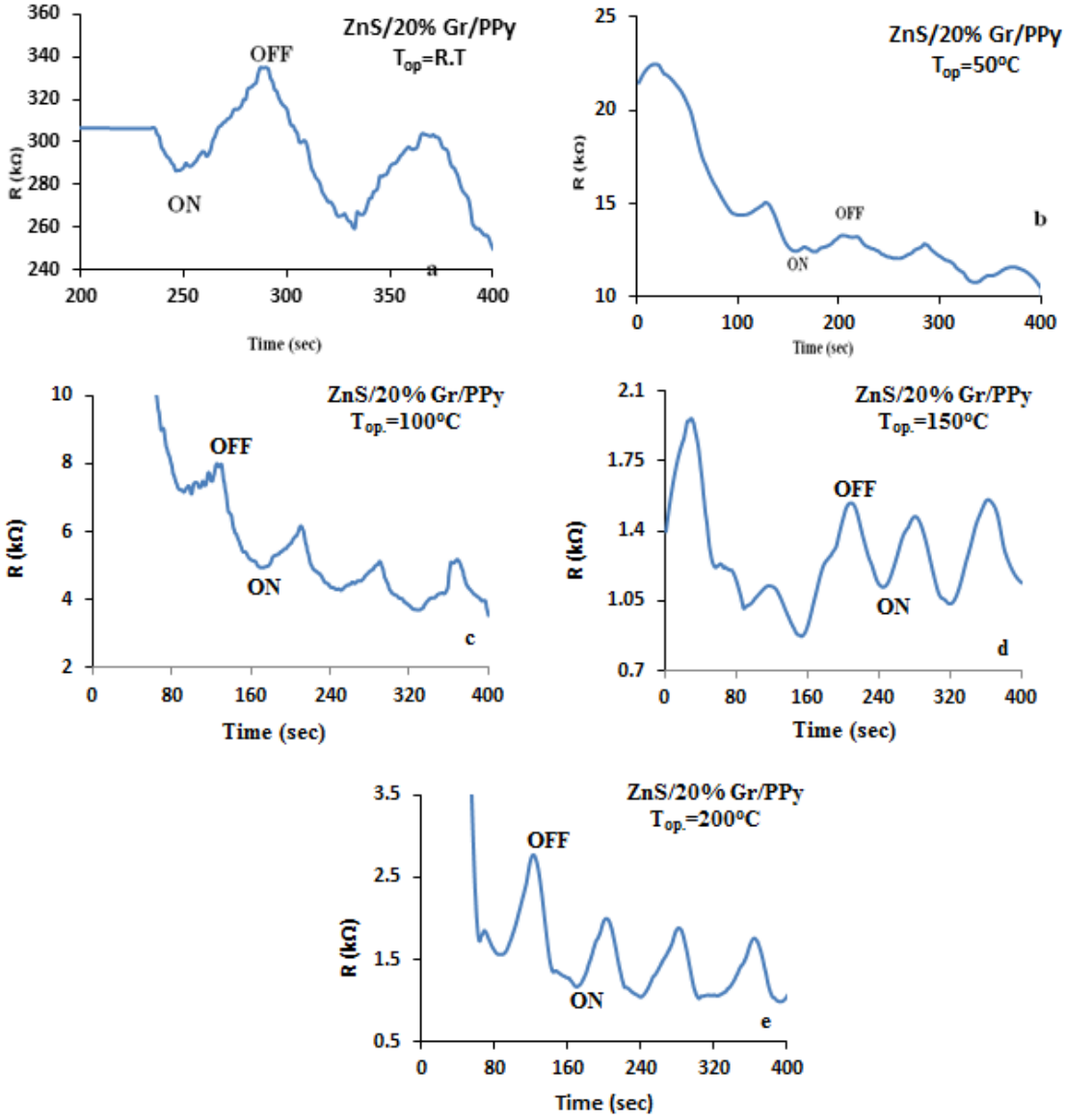

Fig.9: The variation of resistance with time for ZnS/20% Gr/PPy at different operating temperatures against NO_2 gas.

Table 3: Sensitivity% for ZnS / Gr / PPy with different volume ratios (5, 10, 20)% of Gr against NO_2 gas.

Sample	Sensitivity % at				
	30 °C	50 °C	100 °C	150 °C	200 °C
ZnS	0.3	8.6	1.99	- - -	- - -
Gr	9.0	5.2	4.5	- - -	- - -
ZnS / PPy	3.4	14.2	9.0	6.6	4.6
ZnS / 5% Gr / PPy	1.5	3.2	6.2	41.9	- - -
ZnS / 10% Gr / PPy	7	6.4	25.2	39.5	- - -
ZnS / 20% Gr / PPy	27.38	18.81	58.95	41.09	127.09

Table 4: Response time and recovery time of ZnS/Gr/PPy with different volume ratios of Gr against NO_2 gas sensors.

Sample	Res. time (s) / Rec. time (s) at				
	30 °C	50 °C	100 °C	150 °C	200 °C
ZnS	22 / 13	19 / 14	10 / 8	x / x	x / x
Gr	14/16	14/28	8/17	x / x	x / x
ZnS / PPy	14 / 27	26 / 26	26 / 16	17 / 14	35 / 14
ZnS / 5% Gr / PPy	14 / 16	28 / 21	26 / 16	28 / 15	x / x
ZnS / 10% Gr / PPy	26 / 27	27 / 14	26 / 4	23 / 18	x / x
ZnS / 20% Gr / PPy	29 / 29	17 / 36	28 / 27	22 / 20	29 / 12

In general, sensitivity increases slightly with increasing operating temperature but for ZnS / 20% Gr / PPy thin film, the sensitivity increases significantly as shown in Fig.10.

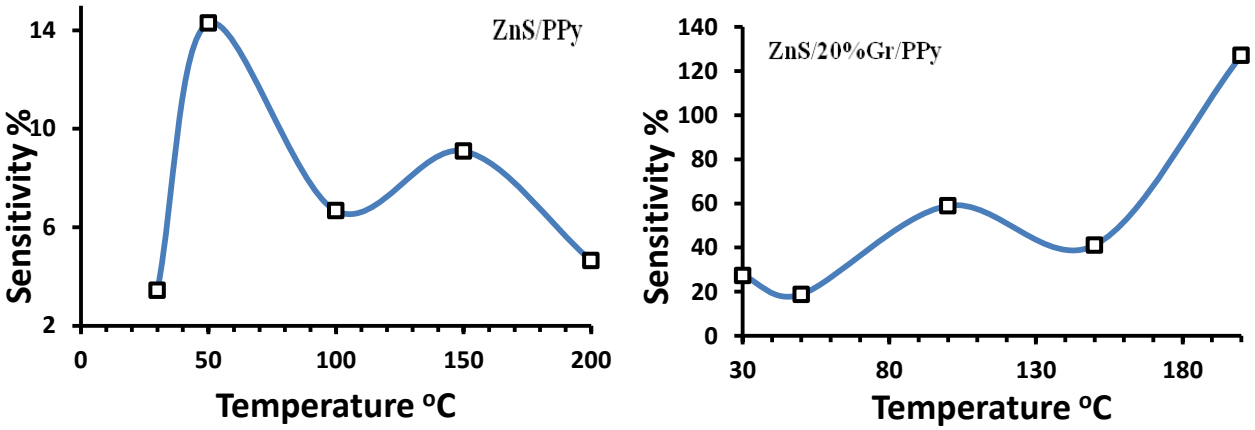

Fig.10: The variation of NO_2 sensitivity with the operating temperature of the ZnS/Gr/PPy with different ratios of ZnS/Gr thin films.

Results show that the sensitivity of the ratio ZnS-PPy decreases with increasing of the operating temperature. The reason for this may be that the surface would be unable to oxidize the gas so intensively and the NO_2 gas may burn before reaching the surface of the film at higher temperature. Thus, the gas sensitivity decreases with increasing temperature [15]. The ratio of ZnS-PPy/ZnS-20% Gr the sensitivity increases with increasing of the operating temperature. It is obvious in Figures an increase in the operating temperature leads to an improvement of the films sensitivity which is attributed to increase in the rate of surface reaction of the target gas because the presence of graphene nanosheet make the exposed area very large to react with gas molecules. Also the appearance of ZnS hexagonal phase may improve the sensitivity to gases.

Conclusions

The pure ZnS and ZnS/Gr have been prepared successfully by a novel method using chemical co-precipitation. X-ray diffraction patterns proved that crystalline system for ZnS is changed from cubic zinc blende structure to hexagonal structure after graphene addition. For gas sensor

device, the maximum sensitivity to NO_2 gas for ZnS-PP/5%Gr of 41.9 % at operating temperatures 150 ^oC and ZnS-PP/20%Gr of 58.95 %, 127% at operating temperatures 100 ^oC, 200 ^oC respectively because the presence of graphene nanosheet and PPy nanotube beside of ZnS nanoparticles.

References

[1] F. Lacy, Lect. Notes Eng. Comput. Sci., 2 (2013) 613-616.
[2] T. Bergstresser and M. Cohen, Physical Review, 164, 3 (1967) 1069-1080.
[3] P. C. Lin, C. C. Hua, T. C. Lee, Journal of Solid State Chemistry, 194 (2012) 282-285.
[4] B.G. Streetman, S. Banerjee, Solid State Electronic Devices, Prentice Hall, fifth ed., 2000.
[5] K. Takahashi, A. Yoshikawa, A. Sandhu, Springer, 2007.
[6] A. K. Geim and K. S. Novoselov, Nature materials, 6 (2007) 183-191.
[7] L. A. Ponomarenko, F. Schedin, M. I. Katsnelson, R. Yang, E. W. Hill, K. S. Novoselov, A. K Geim, Science, 320 (2008) 356-358.
[8] Yuhong Zhou, Daoli Zhang, Jianbing Zhang, Cong Ye, Xiangshui Miao, Journal of Applied Physics, 115 (2014) 073703-1_ 073703-6.
[9] H. J. Yoon, J. H. Yang, Z. Zhou, S. S. Yang, M. M. C. Cheng, Sensors and Actuators B: Chemical, 157, 1 (2011) 310-313.
[10] G. Ko, H. Y. Kim, J. Ahn, Y. M. Park, K. Y., Lee, J. Kim, Current Applied Physics, 10, 4 (2010) 1002-1004.
[11] A. Reung-U-Rai, A. Prom-Jun, W. Prissanaroon-Ouajai, S. Ouajai, Journal of Metals, Materials and Minerals, 18, 2 (2008) 27-31.
[12] K. J. Dunst, K. Cysewska, P. Kalinowski, P. Jasiński, In IOP Conference Series: Materials Science and Engineering, 104, 1 (2016) 1-8.
[13] J. An, J. Liu, Y. Ma, R. Li, M. Li, M. Yu, S. Li, Eur. Phys. J. Appl. Phys. 58, 3 (2012) 1-9.
[14] L. A. Patil, A. R. Bari, M. D. Shinde, V. V. Deo, D. P. Amalnerkar, IEEE Sens. J., 11 (2011) 939-946.
[15] S. A. Garde, Sensors & Transducers Journal, 122, 11 (2010) 128-142.